DOI 10.1007/s10946-015-9509-9
Journal of Russian Laser Research, Volume 36, Number 4, July, 2015

CALCULATION OF THERMAL LENSING IN END-PUMPED YVO_4/Nd:YVO_4 COMPOSITE CRYSTALS IN VIEW OF THE TEMPERATURE DISTRIBUTION

Amir Hossein Farhadian,* Hossein Saghafifar, and Mahdy Dehghanbaghi

Optics & Laser Science & Technology Research Center
Malek-Ashtar University of Technology
Shahinshahr, Iran

*Corresponding author e-mail: Amir_Hossein_Farhadian@yahoo.com

Abstract

Composite crystals are very effective for controlling the thermal effect in end-pumped solid-state lasers. We calculate the temperature-field distribution and thermal focal length in both YVO_4/Nd:YVO_4 and Nd:YVO_4 rectangular crystals with the end-pumped arrangement. Since it is impossible to calculate precisely the thermal focal length in composite crystals directly by the equations, this is usually done by analyzing additional optical path differences (OPD) caused by heat. For this, we use the temperature distributions in OPD calculations. The results show that, at a pump power of 25 W, the maximum temperature on the rear facet of an Nd:YVO_4 original crystal is 560 K, while for the YVO_4/Nd:YVO_4 composite crystal it is 430 K, Also under the same conditions, the thermal focal length in the composite crystal is larger than in the original crystal, as expected.

Keywords: thermal lensing, composite crystal, temperature distribution, OPD.

1. Introduction

End-pumped solid-state lasers have attracted growing attention due to their high efficiency, compact package, and high-beam quality [1, 2]. An Nd:YVO_4 crystal, due to its high absorption coefficient and large stimulated emission cross section, is very suitable for this purpose [3–6]. Despite the suitable optical properties, the weak thermal conduction limits its applications especially in high-power lasers [7–9]. Therefore, the study of thermal effects, such as thermal lensing and thermal stress, as well as their control, is very important. Many methods have been proposed for reducing thermal effects. The use of cooling system and composite crystals [10, 11], design of the resonators with variable configurations [12], and double-end-pumping schemes are some of them [13]. In addition to the thermal problems mentioned above, calculation of the thermal lens is important for laser resonator designing.

The large thermal gradient that arises from the heat deposition in a very small volume near the pumping facet of the laser crystal in the end-pumped system causes thermal lensing and the strongest aberrations at the pumping facet [14]. Low temperature preservation in the crystal body could be adopted to relieve thermal effects and improve laser performance. This can be done by using diffusion bonding of an Nd-doped YVO_4 crystal to a non-doped YVO_4 crystal, which serves as a heat sink for the pumping surface [15].

In this paper, first we analyze the effects of a non-doped crystal on doped-laser crystals in end-pumping configuration, in view of the temperature distribution, and then calculate thermal lensing for both crystals.

Manuscript submitted by the authors in English on December 9, 2014.

 1071-2836/15/3604-0350

2. Temperature Distribution

A part of the absorbed pumping energy is transferred into heat dissipated in the laser crystal due to quantum defects. Using the Cartesian coordinate system, we obtain the temperature distribution in an anisotropic medium solving the steady-state heat-conduction equation [16]

$$k_x \frac{\partial^2 T(x,y,z)}{\partial x^2} + k_y \frac{\partial^2 T(x,y,z)}{\partial y^2} + k_z \frac{\partial^2 T(x,y,z)}{\partial z^2} + q(x,y,z) = 0, \tag{1}$$

where K_x, K_y, and K_z are the thermal conductivities along the x, y, and z directions, T is the temperature, and $q(x,y,z)$ is the heat generated per unit volume. We assume the end-pump configuration of the laser with Gaussian spatial distribution of the laser beam q, which can be expressed approximately as

$$q(x,y,z) = I_0 \exp\left[-2\frac{(x-a/2)^2 + (y-b/2)^2}{w_p^2}\right] \exp(-\alpha z), \qquad I_0 = \frac{2\,\delta P_p \alpha}{\pi w_p^2}[1 - \exp(-\alpha l)], \tag{2}$$

where α is the absorption coefficient, $\delta = 1 - \lambda_p/\lambda_L$ is a quantum defect, w_p is the pump-beam radius, and P_p is the pump power. The YVO_4/Nd:YVO_4 composite crystal employed is shown in Fig. 1.

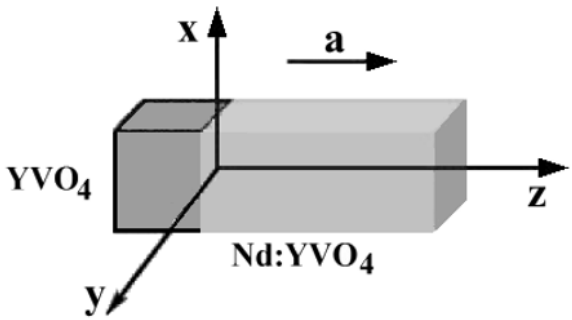

Fig. 1. Schematic of the YVO_4/Nd:YVO_4 composite crystal.

The sizes of a-cut doped Nd:YVO_4 and non-doped YVO_4 crystals are 3×3×5 mm^3 and 3×3×2 mm^3, respectively. The Nd:YVO_4 crystal is wrapped with indium foil and fitted into a copper housing, which is cooled by water at a constant temperature of 289 K. The two-end facets of the composite crystal are in contact with air. The temperature at the surrounding surfaces of the laser crystal is assumed to be the same as the water temperature; thus, the boundary conditions of the thermal model of the original crystal read

$$T(0,y,z) = T(a,y,z) = 289, \qquad T(x,0,z) = T(x,b,z) = 289,$$
$$\frac{\partial T}{\partial z}\,|_{z=0} = h(T - T_{\text{air}}), \qquad \frac{\partial T}{\partial z}\,|_{z=l} = -h(T - T_{\text{air}}).$$

Nevertheless, we should take into account the process of heat transfer between the forward facet of the YVO_4 crystal and the rear facet of the Nd:YVO_4 crystal; thus, the boundary conditions of the composite crystal are

$$T(0,y,z) = T(a,y,z) = 289, \qquad T(x,0,z) = T(x,b,z) = 289,$$
$$T(x,y,0) = T_\mu, \qquad \frac{\partial T}{\partial z}\,|_{z=l} = -h(T - T_{\text{air}}).$$

Here, h is the heat-transfer coefficient between the laser-crystal surface and air, T_{air} is the room temperature (assumed as 300 K), and T_μ is a function of the (x,y) coordinates.

In view of the parameters shown in Table 1, we obtain the temperature distribution in laser crystals solving numerically the heat-conduction equation. As one can see in Fig. 2, the temperature field smoothly rises at the interface between the forward pump face of the YVO_4 crystal and the rear face of the Nd:YVO_4

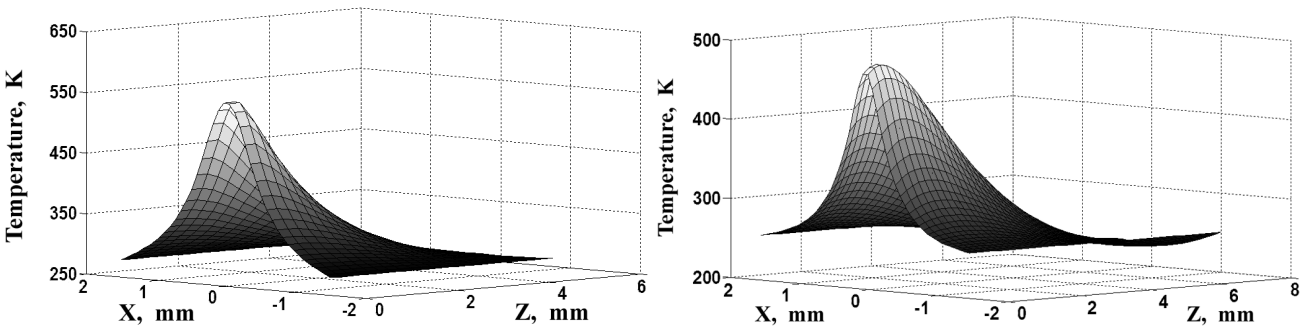

Fig. 2. Temperature distribution in the $x - z$ plane ($y = 0$) at a pump power of 25 W of the original Nd:YVO_4 crystal (left) and the composite YVO_4/Nd:YVO_4 crystal (right).

crystal. This prevents the pump fracture surface from breaking due to a sudden rise in the temperature. Also the relative temperature of the Nd:YVO_4 crystal in the composite crystal increases to a maximum of 430 K, while in a single Nd:YVO_4 crystal it increases to 560 K.

Table 1. Values of the Parameters Used in the Numerical Calculations.

Parameter	Value	Parameter	Value
α	5.32 cm^{-1}	P_p	25 W
$\partial n/\partial T$	$8.5 \cdot 10^{-6}$ k^{-1}	w_p	320 μm
k_x	5.1 $\mathrm{W}^{-1}\cdot\mathrm{m}^{-1}\cdot\mathrm{k}^{-1}$	h	4 $\mathrm{W}\cdot\mathrm{m}^{-2}\cdot\mathrm{k}^{-1}$
k_y	5.23 $\mathrm{W}^{-1}\cdot\mathrm{m}^{-1}\mathrm{k}^{-1}$	T_{air}	300 K
k_z	5.1 $\mathrm{W}^{-1}\cdot\mathrm{m}^{-1}\cdot\mathrm{k}^{-1}$	n_0	2.183
α_T	$4.43 \cdot 10^{-6}$ k^{-1}	ν_{pois}	1

3. Thermal Focal Length

In the case of asymmetric increase in the temperature in a rectangular crystal, thermal lens effect appeared, and it is often characterized by the thermal focal length. The refractive index changes due to the changes in the temperature and mechanical stresses. Also the end-bulging shape of the crystals is very important for creating thermal lensing. Each of these factors causes changes in the optical path difference (OPD) [16], and due to this, we can calculate the thermal focal lens directly from the following equations for changes in the refractive index and the end bulging [16]:

$$f_{\frac{dn}{dT}}(r) = \frac{2\pi K_c w_p^2}{P_p \delta \eta_{\mathrm{abs}} \frac{dn}{dT}} \frac{r^2}{w_p^2\left[1 - \exp\left(-2r^2/w_p^2\right)\right]}, \tag{3}$$

$$f_{\mathrm{bg}}(r) = \frac{2\pi K_c w_p^2}{P_p \delta \eta_{\mathrm{abs}}[(n-1)(\nu_{\mathrm{pois}}+1)\alpha_T]} \frac{r^2}{w_p^2\left[1 - \exp\left(-2r^2/w_p^2\right)\right]}, \tag{4}$$

where α_T, ν_{pois}, and η_{abs} are the thermal expansion coefficient, the Poisson ratio, and the absorption efficiency, respectively. These equations are used frequently in the design of the resonators for original

crystals. Using the values of the parameters shown in Table 2, we calculated the thermal focal length for the Nd:YVO_4 crystal, and the results obtained are shown in Fig. 3.

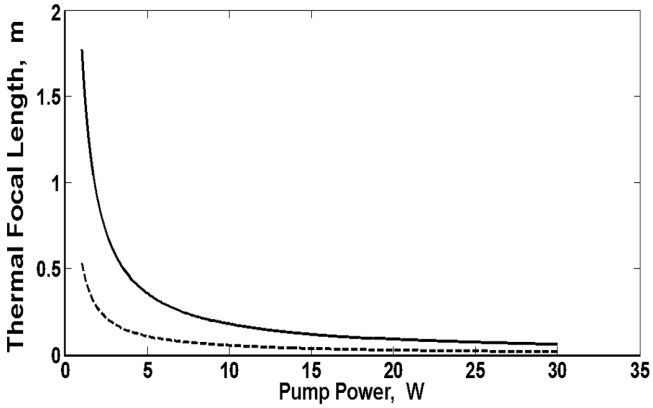

Fig. 3. Thermal focal length for the Nd:YVO_4 crystal due to the changes in the refractive index (dashed curve) and due to the end bulging (solid curve).

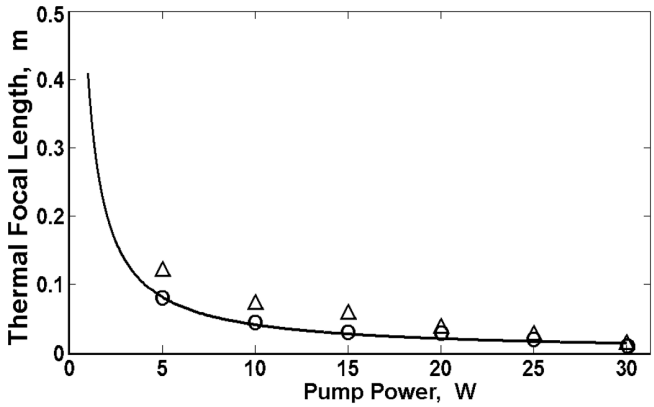

Fig. 4. Thermal focal length due to the OPD for the Nd:YVO_4 crystal (◯) and YVO_4/Nd:YVO_4 crystal (△). Direct calculation is shown by the solid curve.

As we can see in Fig. 3, the end-bulging effect on the total focal length is very small as compared to the refractive index. In order to simulate the thermal effect in composite YVO_4/Nd:YVO_4 crystals, we use the following equation for deriving the focal length of the thermal lens [17]:

$$f(x,y) = (r_e^2)/2[\mathrm{OPD}(0) - \mathrm{OPD}(r_e)], \tag{5}$$

where r_e is the effective radius of the pump light equal to 2ω, with ω being the Gaussian radius of the pump-laser beam, and OPD(0) and OPD(r_e) are the OPD values in the center and at an effective radius of the pump light, respectively. Using a specified thermal distribution, we calculate the OPD from the equation [18]

$$\mathrm{OPD}(x,y) = n_0\alpha_T \int_0^l [T(x,y,z) - T_0]dz + \int_0^l \frac{\partial n}{\partial T} T(x,y)\, dz, \tag{6}$$

where $T(x,y,z)$ is the temperature distribution obtained in the previous section, i.e., it is obtained by a surface fitting toolbox in MATLAB, and polynomials functions are obtained, in view of Eq. (9) and Table 2, namely,

$$\begin{aligned} T \;=\; & p00 + p10*x + p01*y + p20*x\wedge 2 + p11*x*y + p02*y\wedge 2 + p30*x\wedge 3 \\ & + p21*x\wedge 2*y + p12*x*y\wedge 2 + p03*y\wedge 3 + p40*x\wedge 4 + p31*x\wedge 3*y \\ & + p22*x\wedge 2*y\wedge 2 + p13*x*y\wedge 3 + p04*y\wedge 4 + p50*x\wedge 5 + p41*x\wedge 4*y \\ & + p32*x\wedge 3*y\wedge 2 + p23*x\wedge 2*y\wedge 3 + p14*x*y\wedge 4 + p05*y\wedge 5. \end{aligned} \tag{7}$$

According to Eqs. (5)–(7), the thermal focal lens is characterized by the thermal distributions in both crystals that we compare with the results obtained directly from Eqs. (3) and (4); we present this comparison in Fig. 4 at various pump powers.

Table 2. Values of the Parameters Used in the Numerical Calculations of the Fitting Function.

Parameter	Values		Parameter	Values	
	$Nd:YVO_4$ Crystal	$YVO_4/Nd:YVO_4$ Crystal		$Nd:YVO_4$ Crystal	$YVO_4/Nd:YVO_4$ Crystal
p00	2523	635.8	p10	$2.392 \cdot 10^4$	$1.054 \cdot 10^4$
p01	$4.327 \cdot 10^5$	$-2.122 \cdot 10^5$	p20	$2.616 \cdot 10^9$	$-5.554 \cdot 10^8$
p11	$-1.09 \cdot 10^6$	$-1.068 \cdot 10^6$	p02	$-3.745 \cdot 10^8$	$1.144 \cdot 10^7$
p30	$-1.196 \cdot 10^{10}$	$-4.611 \cdot 10^9$	p21	$8.157 \cdot 10^{11}$	$2.228 \cdot 10^{11}$
p12	$-6.347 \cdot 10^8$	$-4.614 \cdot 10^8$	p03	$7.291 \cdot 10^{14}$	$1.918 \cdot 10^{14}$
p31	$7.664 \cdot 10^{11}$	$3.015 \cdot 10^{11}$	p22	$-3.063 \cdot 10^{13}$	$-8.039 \cdot 10^{11}$
p13	$4.689 \cdot 10^{10}$	$5.989 \cdot 10^{10}$	p04	$-3.595 \cdot 10^{13}$	$-1.255 \cdot 10^{12}$
p50	$5.215 \cdot 10^{14}$	$-1.118 \cdot 10^{13}$	p41	$-1.868 \cdot 10^{17}$	$-5.974 \cdot 10^{16}$
p32	$1.423 \cdot 10^{14}$	$1.822 \cdot 10^{14}$	p23	$2.388 \cdot 10^{15}$	$-3.191 \cdot 10^{15}$
p14	$4.524 \cdot 10^{11}$	$-1.754 \cdot 10^{12}$	p05	$2.519 \cdot 10^{15}$	$1.469 \cdot 10^{14}$

The results of calculations of the focal length of the original crystal using the thermal distribution are closed to the results obtained with the help of elaborated equations. The focal length for the composite crystal is larger than in the original crystal. In view of the results obtained, the thermal focal length calculated using the thermal distribution is more precise especially in composite crystals.

4. Conclusions

We investigated numerically the thermal effects in end-pumped solid-state $Nd:YVO_4$ lasers. We analyzed the heat deposition in $Nd:YVO_4$ crystals and $YVO_4/Nd:YVO_4$ composite crystals and compared the temperature field distributions. Also we calculated the thermal focal length in both crystals by direct calculation of the equations elaborated and the temperature distributions. We showed that, in addition to the maximum temperature reduction in composite crystals, the temperature rises smoothly at the surface between YVO_4 and $Nd:YVO_4$ crystals. Also, due to the decrease in the thermal gradient in composite crystals, the thermal focal lens in composite crystals is larger than in the original crystal.

References

1. Y. F. Chen, T. M. Huang, C. L. Wang, and L. J. Lee, *Appl. Opt.*, **37**, 5727 (1998).
2. Y. F. Chen, Y. P. Lan, and S. C. Wang, *Opt. Lett.*, **25**, 1016 (2000).
3. R. Fluck, G. Zhang, U. Keller, et al., *Opt. Lett.*, **21**, 1378 (1996).
4. Z. Cai, W. Wen, J. Yao, et al., *Chin. Opt. Lett.*, **3**, 342 (2005).
5. Y. F. Chen and S. W. Tsai, *IEEE J. Quantum Electron.*, **37**, 580 (2001).
6. P. K. Mukhopadhyaya, M. B. Alsousb, K. Ranganathana, et al., *Opt. Commun.*, **222**, 399 (2003).
7. F. Song, C. Zhang, X. Ding, et al., *Appl. Phys. Lett.*, **81**, 2145 (2002).
8. A. Sugiyama and Y. Nara, *Ceramics Int.*, **31**, 1085 (2005).

9. Z. Ma, D. Li, J. Gao, et al., *Opt. Commun.*, **275**, 179 (2007).
10. M. P. MacDonald, Th. Graf, J. E. Balmer, and H. P. Weber, *Opt. Commun.*, **78**, 383 (2000).
11. Th. Graf, E. Wyss, M. Roth, and H. P. Weber, *Opt. Commun.*, **190**, 327 (2001).
12. A.-Y. Yao, W. Hou, H.-Q. Li, et al., *Chin. Phys. Lett.*, **22**, 607 (2005).
13. H. Ogilvy, M. J. Withford, P. Dekker, and J. A. Piper, *Opt. Express*, **11**, 2411 (2003).
14. H. J. Moon, J. Yi, K. S. Kim, et al., *J. Korean Phys. Soc.*, **33**, 400 (1998).
15. A. Sugiyama and Y. Nara, *Ceramics Int.*, **31**, 1085 (2005).
16. W. Koechner, *Solid-State Lasers Engineering*, William T. Rhodes (2006).
17. Z. G. Li, Z. J. Xiong, W. L. Huang, et al., *Chin. J. Lasers*, **32**, 297 (2005).
18. P. Shi, W. Chen, L. Li, and A. S. Gan, *Appl. Opt.*, **46**, 6655 (2007).